Magnetic exchange interactions and supertransferred hyperfine fields at ^{119}Sn probe atoms in $CaCu_3Mn_4O_{12}$

I. A. Presniakov,[1] V. S. Rusakov,[1] G. Demazeau,[2] A. V. Sobolev,[1] Ya. S. Glazkova,[1] T. V. Gubaidulina,[1] A. M. Gapochka,[1] O. S. Volkova,[1] and A. N. Vasiliev[1]

[1]*Lomonosov Moscow State University, Moscow, 119992 Leninskie Gory, Moscow, Russia*

[2]*ICMCB, CNRS, University Bordeaux 1 "Sciences and Technologies," site de l'ENSCPB 87, Avenue du Dr A. Schweitzer, F-33608 Pessac Cedex, France*

(Received 4 November 2011; published 9 January 2012)

The double manganite $CaCu_3Mn_4O_{12}$ doped with ^{119}Sn atoms (~1 at.% with respect to manganese atoms) was studied by use of Mössbauer spectroscopy. Formally tetravalent Sn^{4+} ions substitute for isovalent manganese ions in the octahedral ($Mn^{4+}O_6$) polyhedra. The covalency effects on the magnetic interactions like superexchange in Cu^{2+}-O-Mn^{4+} and Mn^{4+}-O-Mn^{4+} bonds and supertransferred hyperfine interactions of the ^{119}Sn probe atoms in the manganite structure are discussed. Using a semiquantitative nearest-neighbor cluster model relating the hyperfine magnetic field on the ^{119}Sn nuclei ($H_{Sn} = 105$ kOe at $T = 77$ K) to covalency parameters and angle characterizing the Sn-O-M (M = Cu, Mn) bonds, it has been shown how such an analysis of supertransferred hyperfine interactions of tin probe ions can get fruitful information about strength and sign of the superexchange interactions between Mn^{4+} and Cu^{2+} magnetic ions. A consistent description of the results in the framework of the Weiss molecular field model considering the specific local environment of tin atoms has made it possible to estimate exchange integrals: $J_{CuMn} = -51.1 \pm 0.3$ K and $J_{MnMn} = -0.6 \pm 0.2$ K.

DOI: 10.1103/PhysRevB.85.024406 PACS number(s): 76.80.+y, 75.30.Et, 75.47.Lx

I. INTRODUCTION

The manganite $CaCu_3Mn_4O_{12}$ is the end member in the series of the ferromagnetic perovskites $CaCu_xMn_{7-x}O_{12}$ ($0 \leqslant x \leqslant 3$), which have attracted the interest of the scientific community due to the interplay among their magnetic, electronic, and structural properties.[1,2] These correlations induce various physical phenomena, like colossal magnetoresistance (CMR), multiferroic properties, and colossal dielectric constants that a subject of interest for basic research as well as for practical applications.[1–4]

The correlation of the magnetic and crystallographic structures of $CaCu_3Mn_4O_{12}$ presents several interesting trends. In contrast with most manganites oxides with perovskites-related structures, the corner-shared (MnO_6) octahedra are heavily tilted, which leads to an average Mn-O-Mn bond angle $\vartheta_1 = 142^\circ$.[1] This tilting is induced by the reduction of the 12-fold oxygen coordination of Jahn-Teller Cu^{2+} ions, which are stabilized in a square-coplanar (CuO_4) coordination. Such arrangement gives rise to a complex magnetic topology of superexchange paths, where the ordering results from the competition of the Cu^{2+}-O-Mn^{4+} and Mn^{4+}-O-Mn^{4+} exchange interactions. According to neutron diffraction studies,[5,6] the spins of Cu^{2+} sublattice are aligned antiparallel to those of Mn^{4+} ions forming a common ferromagnetic manganese sublattice. That is a question of the origin of the ferromagnetic (FM) Mn-O-Mn coupling.

Two different situations can be encountered according to the sings of the intrasublattice Mn^{4+}-O-Mn^{4+} couplings. It is well established that Mn-O-Mn bond angle ϑ_1 is a critical factor in determining the nature of magnetic interactions in manganites.[7] According to the Goodenough-Kanamori-Anderson (GKA) rules, the d^3-p^6-d^3 180° superexchange interactions generally lead to antiferromagnetic (AFM) ordering between $Mn^{4+}(d^3)$ magnetic moments (viz., $SrMnO_3$), while 90° superexchange interactions will result in FM ordering. The Mn-O-Mn bond angle $\vartheta_1 = 142^\circ$ in $CaCu_3Mn_4O_{12}$ is nearly at half between 180° and 90°, therefore, the observed ferromagnetic ordering in Mn octahedral sublattice may be related to particular angle dependence of superexchange Mn^{4+}-O-Mn^{4+} interactions. In this case, no frustration effects appear within the Mn^{4+} spins. Another possible cause of the parallel Mn^{4+} spin arrangements may be associated with stronger intersublattice Cu^{2+}-O-Mn^{4+} couplings, which are enhanced due to deviation Cu-O-Mn bond angle $\vartheta_2 = 109^\circ$ from 90° (undistorted perovskites). Assuming all the superexchange interactions are antiferromagnetic with $|J_{CuMn}| > |J_{MnMn}|$ (where J_{CuMn}, $J_{MnMn} < 0$; indirect exchange integrals), the Mn^{4+}-O-Mn^{4+} superexchange couplings will be frustrated: The strength of the Cu^{2+}-O-Mn^{4+} interactions obliges the Mn^{4+} spins, despite a weak AF coupling, to adopt a parallel configuration. Thus, based only on a qualitative analysis, we cannot decide what interactions make the largest contribution to the formation of the magnetic $CaCu_3Mn_4O_{12}$ structure.

In this work, we report the results of the Mössbauer study of the magnetic hyperfine interactions of ^{119}Sn probe atoms in the $CaCu_3Mn_4O_{12}$ lattice. Below Curie temperature ($T < T_C$), the magnetic moments of the Mn^{4+} ($S = 3/2$) and Cu^{2+} ($S = 1/2$) ions produce spin polarization of the ns electrons of the neighboring tin ions via an intermediate O^{2-} ion, which results in Zeeman splitting of the ^{119}Sn Mössbauer spectra. This magnetic hyperfine interaction is measured as the supertransferred hyperfine field (STHF) seen by the ^{119}Sn nucleus. The measurement of the STHF on the ^{119}Sn nucleus is easier because, in this case, except for a small dipolar contribution, it is the only contribution to the observed hyperfine field H_{Sn} value. Since the basic mechanisms of the magnetic supertransferred hyperfine interactions are in many respect analogous to that accepted in the theory of magnetic superexchange interactions, studies of the STHF at the diamagnetic ^{119}Sn atoms can be quite useful in determining the relative importance of the various mechanisms of spin

transfer within the Mn^{4+}-O-Mn^{4+} and Mn^{4+}-O-Cu^{2+} bonds in the manganite structure. Quantitative analysis of the obtained Mössbauer data has been performed with the use of the Weiss local molecular field model in comparison with the magnetic measurements. The mechanisms of inducing hyperfine fields by Mn^{4+} и Cu^{2+} cations, as well as the character of magnetic intra- and intersublattice interactions, have been considered in the framework of the unified approach based on analysis of the overlap symmetry and the degree of filling of the 3*d* orbitals of transition metal cations.

II. EXPERIMENTS

A sample of $CaCu_3Mn_4O_{12}$ containing ~1 at.% (of the total amount of Mn atoms) of ^{119}Sn probe atoms was prepared using a precursor, synthesized in several stages. At the first stage, a homogeneous stoichiometric mixture was prepared from nitrates $Ca(NO_3)_2{\cdot}4H_2O$ and $Cu(NO_3)_2{\cdot}3H_2O$ and manganese nitrate obtained by dissolving manganese metal in dilute nitric acid. The required amount of a solution of ^{119}Sn in diluted nitric acid was added to an aqueous solution of the nitrates. At the second stage, after thorough mixing of the resulting solution, a citric acid excess was added, and the solution was mixed for 15 min. At the final stage, this solution of citrates was evaporated until the formation of an organic rubber, which was first dried at 120 °C and then decomposed in an oxygen flow at 650–700 °C for 12 h.

The homogeneous precursor thus prepared was mixed with $KClO_3$ (20% of the precursor weight) that serves as the *in situ* oxygen source in synthesis at high pressure. This mixture was placed in a platinum capsule and subjected to high pressure (2 GPa) in the reaction cell of a Belt-type of equipment at 1000 °C for 1 h. The product was washed with distilled water to remove the resulting KCl issued from the thermal decomposition of $KClO_3$. X-ray diffraction analysis was performed at 298 K on a STOE diffractometer using CuK_α radiation in the angle range $10^\circ \leqslant 2\vartheta \leqslant 80^\circ$. The magnetization was measured using a superconducting quantum interference device magnetometer MPMS (5T Quantum Design) in a temperature range of 5–400 K at 10 000 G after zero-field cooling.

The ^{119}Sn Mössbauer spectra were recorded in the temperature range 4.4–400 K using a conventional constant acceleration MS-1104Em spectrometer. The radiation source $Ca^{119m}SnO_3$ was kept at room temperature. All isomer shifts refer to the SnO_2 absorber at 300 K. The values for the hyperfine magnetic fields H_{Sn} at ^{119}Sn nuclei were obtained using values of 23.8795 keV for the γ-ray energy and the $g_{gr} = -2.09456$ and $g_{ex} = +0.422$ values for the ground and excited states. The experimental Mössbauer spectra were analyzed using the methods of spectral simulation and reconstruction of the distribution of hyperfine parameters of partial spectra, which were realized in the MSTOOLS software package.[8]

III. RESULTS

A. X-ray diffraction data

The x-ray diffraction data (XRD) pattern of the synthesized sample indicates the formation of $CaCu_3Mn_{3.96}{}^{119}Sn_{0.04}O_{12}$ and a small amount of a CuO impurity phase. The lattice parameter of the cubic cell [$a = 7.2321(7)$ Å] obtained as a result of indexing the XRD pattern (space group $Im\bar{3}$) differs slightly from the corresponding value $a = 7.22793(6)$ Å for the Sn-undoped $CaCu_3Mn_4O_{12}$ sample.[9] Such a difference between the unit-cell parameters is consistent with the corresponding data for the isostructural perovskite $CaCu_3Sn_4O_{12}$ [$a = 7.64240(8)$ Å][10] where Sn^{4+} ions (0.69 Å) fully substitute for Mn^{4+} ions (0.53 Å) having the same valence but a smaller size.

B. Mössbauer and magnetic data

The ^{119}Sn Mössbauer spectrum of the tin-doped $CaCu_3Mn_{3.96}{}^{119}Sn_{0.04}O_{12}$ sample measured at $T = 77$ K ($\ll T_C$) can be described as a superposition of paramagnetic and magnetic components [Fig. 1(a)].

In order to choose a model for representing such a spectrum, we reconstructed two distribution functions of hyperfine parameters: the quadrupole splittings $p(\Delta)$ for the paramagnetic contribution [Fig. 1(b)] and the magnetic hyperfine fields $p(H_{Sn})$ for the magnetic contribution [Fig. 1(c)].[8,11] A comparative analysis of the $p(\Delta)$ and $p(H_{Sn})$ profiles allows

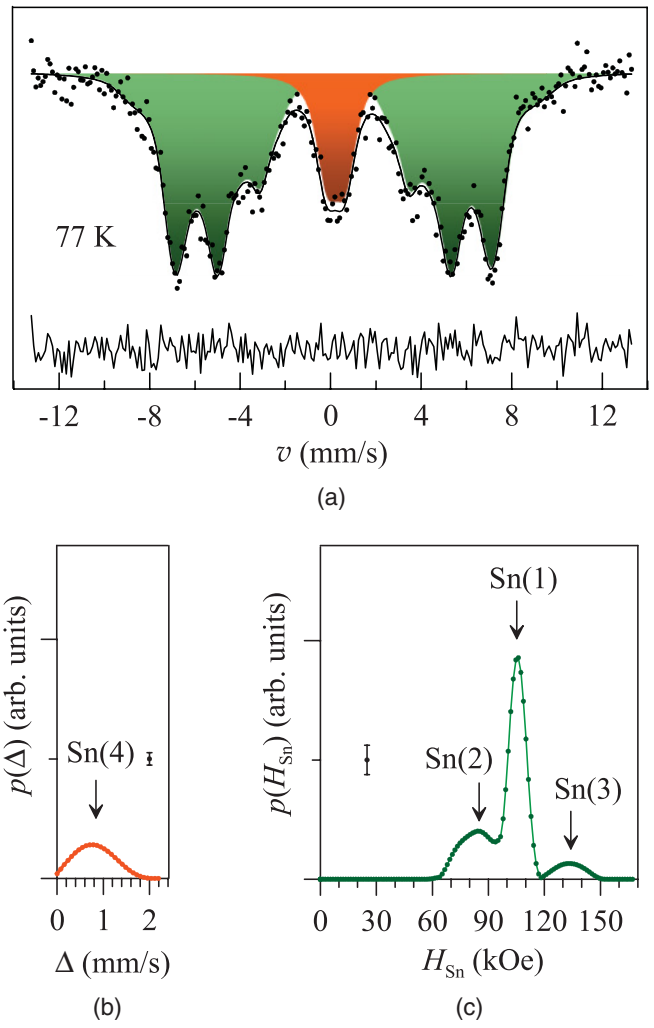

FIG. 1. (Color online) ^{119}Sn Mössbauer spectrum of the sample $CaCu_3Mn_{3.96}{}^{119}Sn_{0.04}O_{12}$ recorded at $T = 77$ K (a); distribution functions of the quadrupole splitting $p(\Delta)$ (b) and the hyperfine magnetic field $p(H_{Sn})$ (c).

us to assume that the tin atoms occupy three magnetically nonequivalent positions with the average magnetic hyperfine fields $\bar{H}_{\mathrm{Sn}(1)} = 105$ kOe, $\bar{H}_{\mathrm{Sn}(2)} = 86$ kOe, and $\bar{H}_{\mathrm{Sn}(3)} = 123$ kOe, which may correspond to one (only manganite) or several (manganite+impurity phase) magnetic phases. As shown below, the paramagnetic component with the average quadrupole splitting $\bar{\Delta}_{\mathrm{Sn}(4)} = 0.4$ mm/s [Fig. 1(b)] can be related with one of the nonmagnetic tin impurity phases.

Based on the results of the $p(\Delta)$ and $p(H_{\mathrm{Sn}})$ profile analysis, we described a series of spectra measured at $T \ll T_C$ (where the resolved magnetic structure persists) as a superposition of three Zeeman sextets and one unresolved quadrupole doublet (Fig. 2). The best-fit hyperfine parameters and relative intensities (I_i) partial spectra are listed in Table I.

To reveal the character of the change in the Mössbauer spectra corresponding to the expected magnetic phase transition range of the sample, we carried out measurements in the temperature range 300–360 K, which includes the Curie temperature ($T_C = 355$ K) of the tin-undoped $CaCu_3Mn_4O_{12}$ manganite. In this temperature range, the spectra represent a poorly resolved magnetic structure below the Curie point and a slightly asymmetric paramagnetic structure above this point (Fig. 3). To determine the magnetic phase transition temperature, we reconstructed magnetic hyperfine field distributions $p(H_{\mathrm{Sn}})$ (Fig. 4). From the temperature dependencies of the mean field $\bar{H}_{\mathrm{Sn}}(T)$ and dispersion $D_{p(H_{\mathrm{Sn}})}$ of the resulting distributions, we determined the temperature at which the magnetic hyperfine structure of the spectra completely disappears (Fig. 5). The resulting temperature 337±3 K coincides with the Curie temperature $T_C = 336 \pm 1$ K determined by the Arrott method from the H/M versus M^2 plot (inset in Fig. 5).

IV. MODEL CALCULATION OF THE SUPERTRANSFERRED HYPERFINE FIELDS AT ^{119}Sn NUCLEI

A. Local environment and electronic state of the Cu^{2+} and Mn^{4+} cations in the $CaCu_3Mn_4O_{12}$ structure

At any temperature, the manganite $CaCu_3Mn_4O_{12}$ has a cubic structure (space group $Im\bar{3}$) with an ordered distribution of Ca^{2+} and Cu^{2+} ions forming two different crystallographic sublattices (Fig. 6). Spherically symmetric Ca^{2+} ions form slightly distorted dodecahedra (CaO_{12}). The Jahn-Teller ions $Cu^{2+}(3d^9)$ are located in distorted polyhedra (CuO_{12}), where three sets of Cu-O distances (r_i) are observed: $r_1 = 1.90$ Å, $r_2 = 2.80$ Å, and $r_3 = 3.20$ Å.[9] The difference in the Cu-O distances is so strong that the Cu^{2+} ions can be conventionally thought of as having a square (CuO_4) oxygen environment with the bond lengths $\langle r \rangle = 1.90$ Å. In the local coordinate system (x, y, z) of the Cu^{2+} ion [Fig. 7(a)] its single unpaired electron is located on the $d_{x^2-y^2}$ (b_{1g}) orbital, whereas other 3d orbitals (e_g, a_{1g}, b_{2g}) are completely filled [Fig. 7(b)]. The Mn^{4+} ($3d^3$) ions forming the B sublattice are in almost undistorted oxygen octahedra (MnO_6). Three unpaired electrons of the manganese ion in its local coordinate system (x', y', z') are located on the $d_{x'z'}$, $d_{y'z'}$, $d_{x'y'}$ (t_{2g}) orbitals, while two degenerate orbitals, $d_{z'^2}$ and $d_{x'^2-y'^2}$(e_g), remain vacant.

In the $CaCu_3Mn_4O_{12}$ structure each octahedral Mn^{4+} ion is linked with each other by six Mn^{4+}-O-Mn^{4+} bonds in an

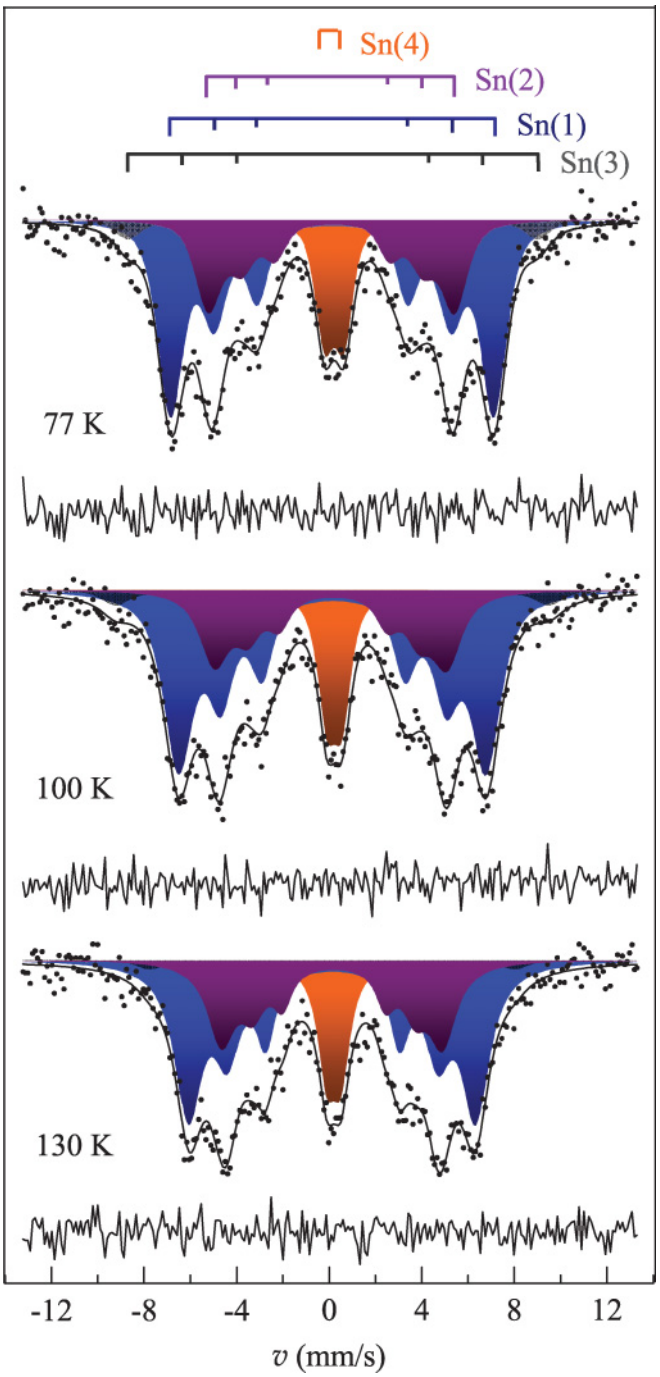

FIG. 2. (Color online) Modeling reconstruction of ^{119}Sn Mössbauer spectra of the sample $CaCu_3Mn_{3.96}{}^{119}Sn_{0.04}O_{12}$ recorded at temperatures $T \ll T_C$.

octahedral sublattice (Fig. 6). In addition, each Mn^{4+} ion has six square polyhedra (CuO_4) in its nearest environment, which are linked through a shared oxygen ion by Mn-O-Cu bonds. The ordering of the Ca^{2+} and Cu^{2+} ions leads to a cooperative rotation of all (MnO_6) polyhedra; as a result, the Mn-O-Mn angle (ϑ_1) decreases from 180° (as in the cubic perovskite structure) to 140°, while the Mn-O-Cu angle (ϑ_2) increases from 90° to 109° [Fig. 7(a)]. These changes in the ϑ_1 and ϑ_2 angles has a significant effect on both intrasublattice Mn^{4+}-O-Mn^{4+} and intersublattice Cu^{2+}-O-Mn^{4+} exchange coupling.

TABLE I. Hyperfine parameters of partial ^{119}Sn Mössbauer spectra of manganite $CaCu_3Mn_{3.96}{}^{119}Sn_{0.04}O_{12}$.

T (K)	Partial spectrum	δ (mm/s)	E[a] (mm/s)	H_{Sn} (kOe)	I (%)
77	Sn(1)	0.15 ± 0.02	-0.01 ± 0.02	104.9 ± 0.2	55.8 ± 2.5
	Sn(2)	0.13 ± 0.04	-0.02 ± 0.03	79.9 ± 0.6	25.6 ± 1.2
	Sn(3)	0.15	0	133.0 ± 2.4	5.7 ± 0.6
	Sn(4)	0.22 ± 0.02	0.42 ± 0.02	—	12.9 ± 0.3
100	Sn(1)	0.16 ± 0.02	-0.03 ± 0.02	99.8 ± 0.3	58.1 ± 2.4
	Sn(2)	0.13 ± 0.05	-0.06 ± 0.03	75.4 ± 0.8	24.1 ± 1.3
	Sn(3)	0.14	0	140.8 ± 3.0	4.9 ± 0.6
	Sn(4)	0.23 ± 0.02	0.33 ± 0.02	—	12.9 ± 0.3
130	Sn(1)	0.14 ± 0.02	-0.01 ± 0.02	93.1 ± 0.3	55.0 ± 2.6
	Sn(2)	0.17 ± 0.03	-0.04 ± 0.03	71.8 ± 0.7	28.7 ± 1.7
	Sn(3)	0.14	0	118.6 ± 4.9	3.3 ± 0.7
	Sn(4)	0.21 ± 0.02	0.31 ± 0.02	—	13.0 ± 0.3

[a]$\varepsilon = \frac{1}{2}\Delta$ for the paramagnetic partial spectrum of Sn(4); Δ is the quadrupole splitting.

B. Partial contributions of the Mn^{4+} and Cu^{2+} cations to the STHF at the ^{119}Sn nuclei

In the perovskite-like $CaCu_3Mn_4O_{12}$ oxide, diamagnetic ^{119}Sn probe atoms are bound to the nearest Mn^{4+} and Cu^{2+} magnetic cations through oxygen anion; therefore, the magnetic hyperfine field at the ^{119}Sn nuclei (H_{Sn}) appears as a result of the overlapping of electron shells and spin transfer in the Sn-O-Mn and Sn-O-Cu chains. To estimate the sign and magnitude of the partial contribution to the H_{Sn} value from each of the six Mn^{4+} (h_{Mn}) and Cu^{2+} (h_{Mn}) cations surrounding tin ions, we used the cluster method of molecular orbitals, which was previously used for calculating

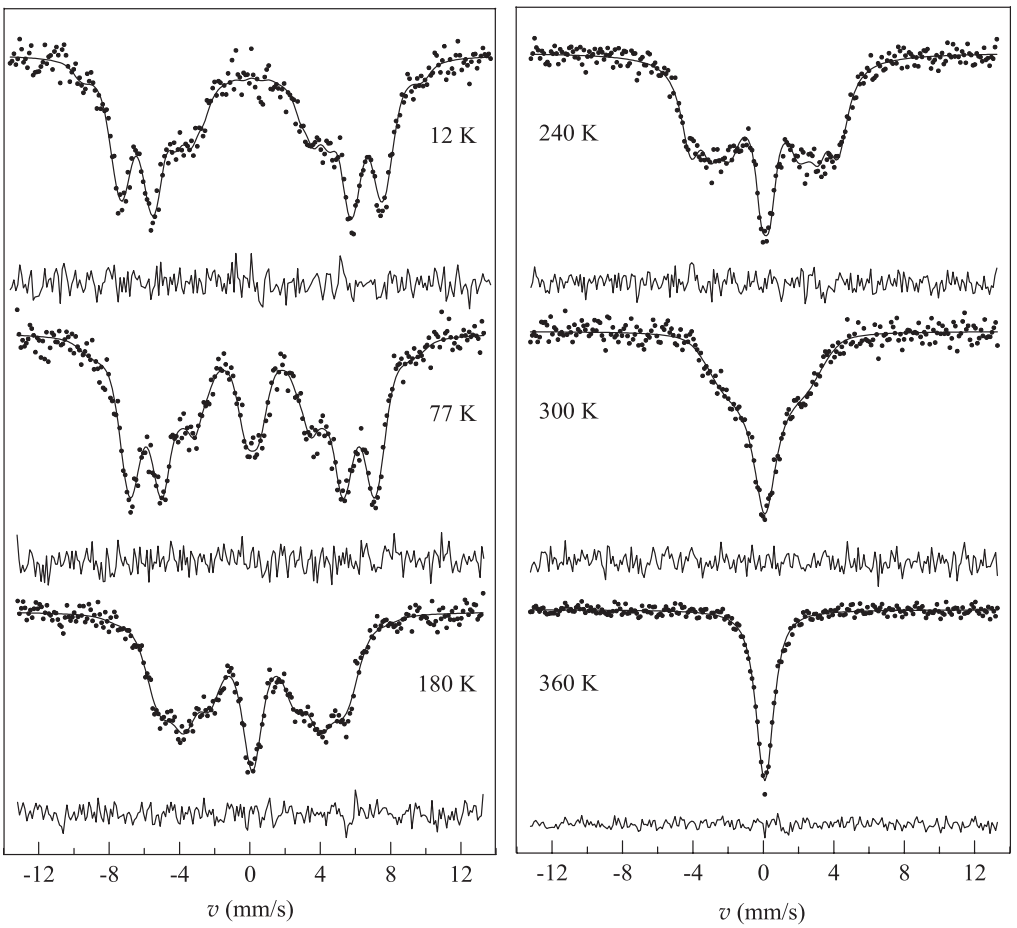

FIG. 3. Characteristic ^{119}Sn Mössbauer spectra of $CaCu_3Mn_{3.96}{}^{119}Sn_{0.04}O_{12}$ in the temperature range around the Curie temperature ($T_C = 335 \pm 3$ K).

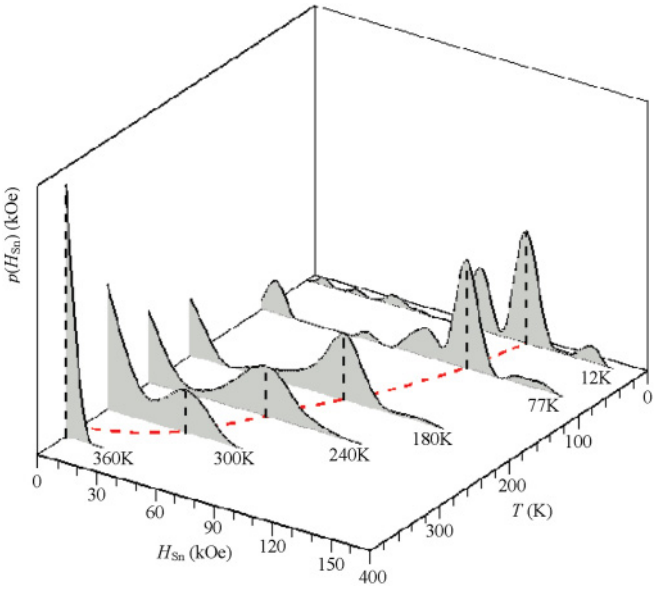

FIG. 4. (Color online) Distributions $p(H_{Sn})$ of hyperfine magnetic fields at ^{119}Sn nuclei in the $CaCu_3Mn_{3.96}{}^{119}Sn_{0.04}O_{12}$ manganite at various temperatures.

the magnetic hyperfine fields at the nuclei of ^{57}Fe and ^{119}Sn atoms in different magnetically ordered compounds.[12–14]

The calculations were performed with inclusion of two bonding molecular orbitals (see the appendix) localized in the {Sn-6O-(6Mn, 6Cu)} cluster in which the angles in Sn^{4+}-O-Mn^{4+} (ϑ_1) and Sn^{4+}-O-Cu^{2+} (ϑ_2) were taken to be equal to the corresponding values for the Mn-O-Mn ($\vartheta_1 = 142^\circ$) and Mn-O-Cu ($\vartheta_2 = 109^\circ$) in tin undoped manganite $CaCu_3Mn_4O_{12}$.[9]

According to the theory developed in Refs. 12–14, the partial field h_{Mn} induced by one $Mn^{4+}(t_{2g}^3 e_g^0)$ cation can be conventionally represented by a superposition of the contributions h_{Mn}^{σ} and h_{Mn}^{π} that are caused by the involvement of both: the empty e_g orbitals (σ bonds) and the half-filled t_{2g} orbitals (π bonds) of Mn^{4+} cations in the spin polarization of the ns electrons of the neighboring tin ions via an intermediate O^{2-} ion. These contributions can be calculated by use of the following equations:[12–14]

$$h_{Mn}^{\sigma} = 525(N_O^{\uparrow}N_O^{\downarrow})^2\left(-\sum_{n=1}^{4} s_{ns}\varphi_{ns}(0) + b_{5s}\varphi_{5s}(0)\right)^2 \times [(a_{\sigma,Mn}^{\uparrow})^2 - (a_{\sigma,Mn}^{\downarrow})^2]\cos^2\vartheta_1, \quad (1a)$$

$$h_{Mn}^{\pi} = 525(N_O^{\uparrow}N_O^{\downarrow})^2\left(-\sum_{n=1}^{4} s_{ns}\varphi_{ns}(0) + b_{5s}\varphi_{5s}(0)\right)^2 \times (a_{\pi,Mn}^{\uparrow})^2\sin^2\vartheta_1, \quad (1b)$$

where $s_{ns} = \langle p_z | ns\rangle$ are the pair overlap integrals of the ns orbitals of Sn^{4+} cation with the $2p$ orbital of O^{2-} anion in the Sn^{4+}-O bonds; b_{5s} is the covalency parameter describing the electron transfer from the $2p$ orbital of O^{2-} anion into an empty $5s$ orbital of Sn^{4+} cation; $(a_{\sigma,Mn}^{\uparrow(\downarrow)})^2$ and $(a_{\pi,Mn}^{\uparrow})^2$ are the covalence parameters for individual σ- and π- Mn^{4+}-O bonds, that depend on the direction $\uparrow(\downarrow)$ of the Mn^{4+} spin (hereafter, the positive direction is that of the spins of the Mn^{4+} cations surrounding Sn^{4+}); $\varphi_{ns}(0)$ stands for the wave functions of ns orbitals ($n = 1$–5) at the nuclei of Sn^{4+} cations;[15] and $N_O^{\uparrow}$ and $N_O^{\downarrow}$ are normalizing constants for the corresponding directions of electron spins localized in the $2p$ orbitals of oxygen anions (the expressions for them were reported in Refs. 13 and 14).

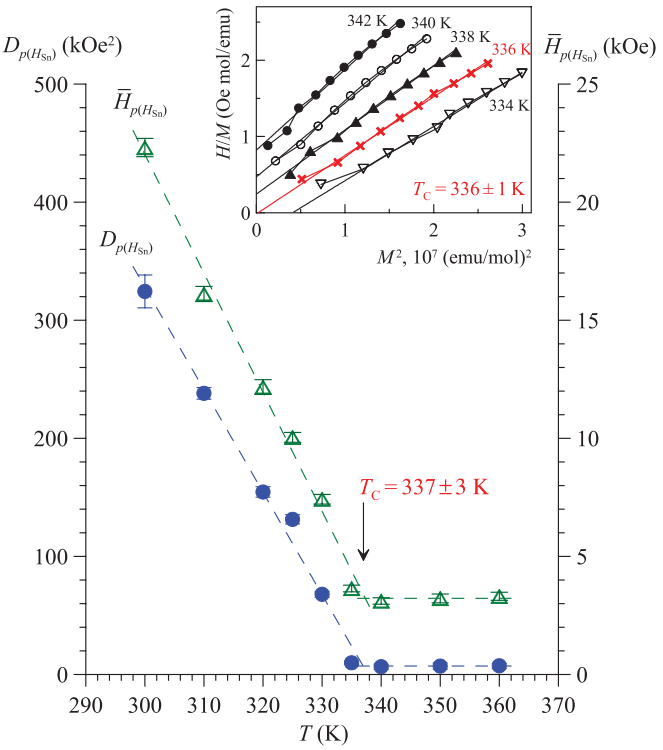

FIG. 5. (Color online) Temperature dependencies of the mean field $\overline{H}_{p(H_{Sn})}$ and dispersion $D_{p(H_{Sn})}$ of the distributions $p(H_{Sn})$. The inset present the result of our analysis of the magnetic measurements for a $CaCu_3Mn_{3.96}{}^{119}Sn_{0.04}O_{12}$ sample by the Arrott method.

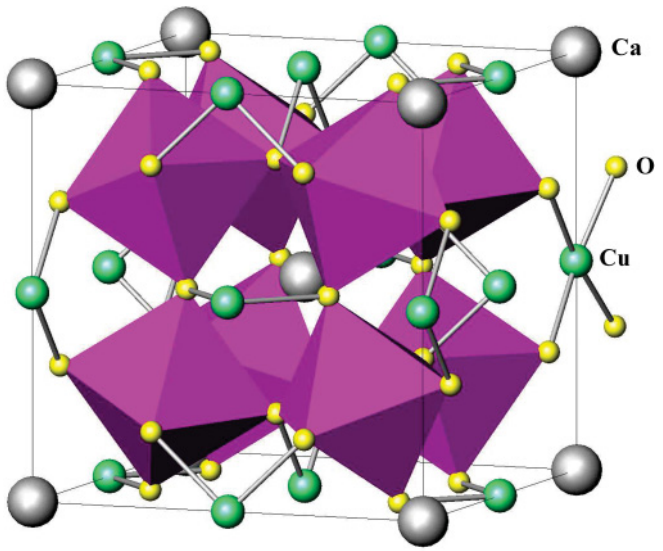

FIG. 6. (Color online) Crystal structure of manganite $CaCu_3Mn_4O_{12}$ (the octahedra shown in the figure are centered by Mn^{4+} cations).

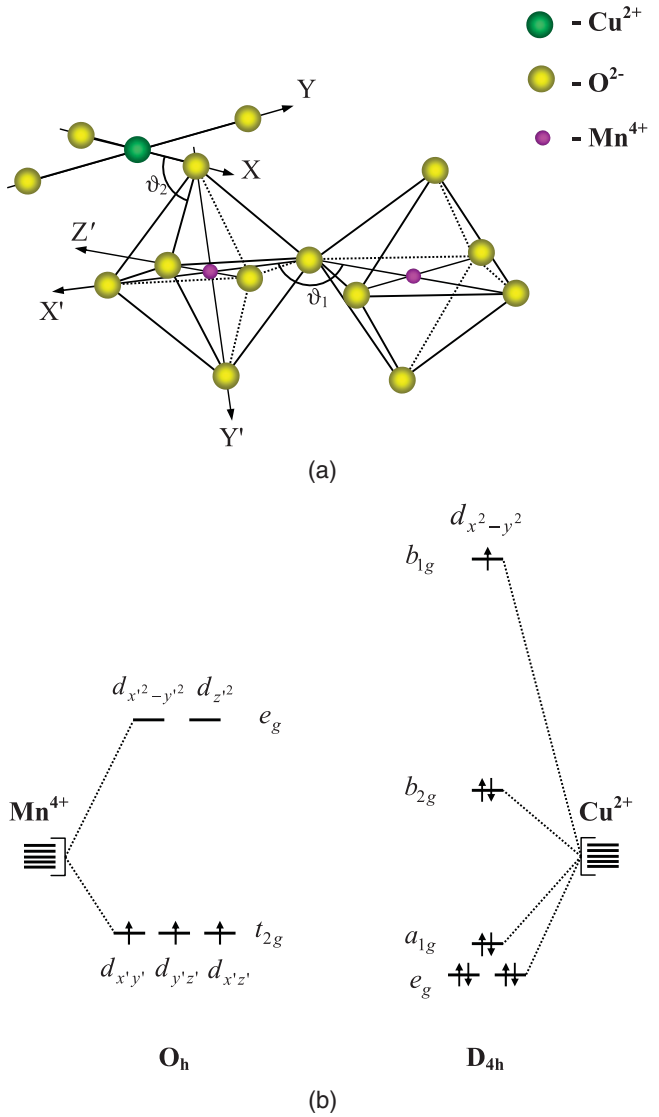

FIG. 7. (Color online) Schematic representation of the nearest environments (a) and the energy diagrams for the Mn^{4+} (b) and Cu^{2+} (c) in manganite $CaCu_3Mn_4O_{12}$.

There are no reliable computational methods to independently determine the b_{5s}, $(a^{\uparrow(\downarrow)}_{\sigma,\mathrm{Mn}})^2$ and $(a^{\uparrow}_{\pi,\mathrm{Mn}})^2$ parameters entering Eq. (1). Therefore, to estimate the first of them (b_{5s}), we used the equation relating this parameter to the population of the 5*s* orbital (n_{5s}) of the octahedrally coordinated Sn^{4+} cations:

$$b_{5s} = \left(\frac{1}{6}\frac{n_{5s}}{(N^{\uparrow}_{\mathrm{O}})^2 + (N^{\downarrow}_{\mathrm{O}})^2}\right)^{1/2}. \quad (2)$$

The n_{5s} value was obtained from the expression for the isomer shift δ_{Sn} as a function of populations of the atomic 5*s* and 5*p* orbitals of the tin cations:[16]

$$\delta_{\mathrm{Sn}}(300\,\mathrm{K}) = -0.433 + 3.01n_{5s} - 0.20n_{5s}^2 - 0.17n_{5s}n_{5p}. \quad (3)$$

The valence orbitals of the octahedrally coordinated Sn^{4+} cations formally belong to the sp^3d^2 hybrid state; therefore, we can assume that $n_{5p} = 3n_{5s}$. In this case, the substitution of the experimental value $\delta_{\mathrm{Sn}}(300\,\mathrm{K}) = 0.09$ mm/s into Eq. (3) allowed us to determine the population $n_{5s} = 0.182$ for the Sn^{4+} probe cations in the $CaCu_3Mn_4O_{12}$ structure. The substitution of this value into Eq. (2) leads to the charge transfer integral, $b_{5s} = 0.161$.

The highest uncertainty in the estimation of the h^{σ}_{Mn} and h^{π}_{Mn} contributions is associated with the choice of the covalence parameters $(a^{\uparrow(\downarrow)}_{\sigma,\mathrm{Mn}})^2$ and $(a^{\uparrow}_{\pi,\mathrm{Mn}})^2$, which have a considerable effect on computation results [see Eq. (1)]. To estimate these parameters, we used the results of earlier Mössbauer studies of magnetic hyperfine interactions at the nuclei of ^{119}Sn probe atoms in $Sr_{1-x}Ca_xMnO_3$ solid solutions.[17,18] According to structural data, a change in the composition of these compounds leads to a monotonic change in the angle ϑ of the Mn-O-Mn chains, and the Mn^{4+}-O bond lengths remaining unaltered, $r_{\mathrm{Mn-O}} = 2.01$ Å.[19] Analysis of the hyperfine fields H_{Sn} for solid solutions of various composition showed[18] that the angular dependence $H_{\mathrm{Sn}}(\vartheta)$ is described by the following equation:

$$H_{\mathrm{Sn}}(\vartheta) = H_{180}\cos^2\vartheta + H_{90}\sin^2\vartheta, \quad (4)$$

where $H_{180} = -20$ kOe and $H_{90} = 609$ kOe are the hyperfine field values at $\vartheta = 180^\circ$ and 90°, respectively. The substitution of the H_{180} and H_{90} values into Eq. (1), as well as taking into account the dependence of the covalence parameters on the Mn^{4+}-O bond length $a^2_{\sigma,\mathrm{Mn}} \propto 1/r^7_{\mathrm{Mn-O}}$,[20] allowed us to calculate the parameters expected for $CaCu_3Mn_4O_{12}$ ($r_{\mathrm{Mn-O}} = 1.915$ Å)[21]: $(a^{\uparrow}_{\pi,\mathrm{Mn}})^2 = 0.167$ and $(a^{\uparrow}_{\sigma,\mathrm{Mn}})^2 - (a^{\downarrow}_{\sigma,\mathrm{Mn}})^2 = -0.008$ (the negative sign means that spin density with predominantly positive spin direction (↑) is transferred to the vacant e_g orbitals).

Substituting the corresponding values of the b_{5s}, $(a^{\uparrow}_{\pi,\mathrm{Mn}})^2$, and $(a^{\uparrow}_{\sigma,\mathrm{Mn}})^2 - (a^{\downarrow}_{\sigma,\mathrm{Mn}})^2$ parameters into Eq. (1), we obtain the partial contributions $h^{\sigma}_{\mathrm{Mn}} = -2.9$ kOe and $h^{\pi}_{\mathrm{Mn}} = 37.2$ kOe to the magnetic hyperfine field at the ^{119}Sn nuclei induced by one Mn^{4+} cation.

Using an analogous computational scheme, we calculate the partial contribution h_{Cu} to the hyperfine field H_{Sn} from one Cu^{2+} cation:

$$h^{\sigma}_{\mathrm{Cu}} = 525(N^{\uparrow}_{\mathrm{O}}N^{\downarrow}_{\mathrm{O}})^2\left(-\sum_{n=1}^{4} s_{ns}\varphi_{ns}(0) + b_{5s}\varphi_{5s}(0)\right)^2 \times (a^{\downarrow}_{\sigma,\mathrm{Cu}})^2\cos^2\vartheta_2. \quad (5)$$

As in the case of calculation of h_{Mn} contribution, there is the highest uncertainty in choosing of the covalence parameter $(a^{\downarrow}_{\sigma,\mathrm{Cu}})^2$ of the σ bond Cu^{2+}-O. Inasmuch as no information on the covalence parameter $(a^{\downarrow}_{\sigma,\mathrm{Cu}})^2$ is available, we used the corresponding value for the σ bond Fe^{3+}-O $(a^{\uparrow}_{\sigma,\mathrm{Fe}})^2 = 0.28$, determined for Fe^{3+} cations in the tetrahedral environment with $r_{\mathrm{Fe-O}} = 1.89$ Å,[12] which is close to $r_{\mathrm{Cu-O}} = 1.91$ Å.[9] Close values of the $(a^{\downarrow}_{\sigma,\mathrm{Cu}})^2$ and $(a^{\uparrow}_{\sigma,\mathrm{Fe}})^2$ parameters (provided that $r_{\mathrm{Cu-O}} \approx r_{\mathrm{Fe-O}}$) are confirmed by estimates of these parameters with the use of the relation $a^{\downarrow(\uparrow)}_{\sigma} \propto t_{pd\sigma}/\Delta$, where $t_{pd\sigma}$ is the resonance integral [$t_{pd\sigma}(Fe^{3+}\text{-O}) = 1.5$–$1.8$ eV, $t_{pd\sigma}(Cu^{2+}\text{-O}) = 1.3$–$1.5$ eV][22] and $\Delta_{\sigma} = (\varepsilon_d - \varepsilon_p)$ is the difference between the one-electron energies of the $2p_{\sigma}$ orbitals of the O^{2-} anion (ε_p) and the 3*d* orbitals (ε_d) of the

Cu^{2+} cation of the corresponding transition metal ($\Delta^{Fe} = 3$–4.5 eV, $\Delta^{Cu} = 2.2$–3 eV).[22] The substitution of the values of all necessary parameters into Eq. (5) gives the partial contribution to the hyperfine field from one Cu^{2+} cation, $h^{\sigma}_{Cu} = -17.4$ kOe.

Note that the values of the bond covalence parameters (which introduce the main error) used in the model calculations of partial contributions h^{σ}_{Mn}, h^{π}_{Mn}, and h^{σ}_{Cu} are determined accurately to a percentage except for parameter $(a^{\downarrow}_{\sigma,Cu})^2$, which has an error that is significantly higher. Thus, we expect that the calculation error reaches 10%. Therefore, the combinations of the partial contributions that will be compared to experimental date are given as accurate to the first two significant digits.

V. DISCUSSION

A. Supertransferred hyperfine fields at ^{119}Sn probe atoms

The isomer shift δ values of the four components (in the range 0.13–0.22 mm/s) correspond to the tin atoms in the formal oxidation state +4 with an octahedral oxygen environment.[16] Since the ^{119}Sn Mössbauer spectra shown in Fig. 1 were recorded well below the magnetic ordering temperature $T \ll T_C$ of the tin-doped $CaCu_3Mn_4O_{12}$ sample, the weak paramagnetic component Sn(4) (Table I) corresponds to the Sn^{4+} ions stabilized in one of the nonmagnetic impurity oxide phases (including tin phases) which was not detected in the x-ray diffraction pattern.

An analysis of the temperature dependence of the dispersion $D_{p(HSn)}$ for distribution $p(H_{Sn})$ demonstrates that the major magnetic contribution to the experimental spectra vanishes at a temperature of ~337 K (Fig. 5), which is close to the Curie temperature $T_C = 355$ K of Sn-undoped manganite.[4] This result seems to be independent experimental evidence for the stabilization of the most Sn^{4+} ions in the magnetically ordered $CaCu_3Mn_4O_{12}$ matrix. The lower value of this temperature as compared with T_C can be due to magnetic dilution, which leads to the rupture by tin atoms of the magnetically active Cu-O-Mn and Mn-O-Mn bonds. It should be noted that an analogous decrease in magnetic ordering temperature was previously observed when ^{57}Fe atoms were introduced into the structure of $CaCu_3Mn_4O_{12}$.[23] However, in this case, the most probable reason for a decrease in T_C is connected with specifics of the charge compensation of impurity Fe^{3+} ions leading to the stabilization of a small amount of Mn^{3+} ions in the A' sublattice.[23]

The weakest magnetic component Sn(3), which is not observed in the spectra at higher temperatures, can be assigned to Sn^{4+} cations stabilized in any of the magnetic impurity phases ($CaMn_2O_4$, Mn_3O_4, Mn_2O_3, and so on) or located at the surface of manganite grains. Taking into account that the contribution of the Sn(3) component is small (with the relative intensity $I_{Sn(3)} \sim 5\%$, Table I), it is difficult to accurately determine its hyperfine parameters; therefore, the behavior of this contribution is not discussed in the following parts.

The major magnetic components of the spectra are Sn(1) and Sn(2) (Table I). Since the magnetic contribution vanishes at a temperature close to the Curie temperature of the undoped manganite, both components Sn(1) and Sn(2) correspond to tin atoms stabilized in the $CaCu_3Mn_4O_{12}$ structure.

The Sn^{4+} cations are known to be always stabilized in positions with octahedral oxygen coordination, which is due to their size and specifics of their spherically symmetric electronic configuration $3d^{10}4s^0$. Therefore, we can assume that, in the structure of manganite $CaCu_3Mn_4O_{12}$, the Sn^{4+} probe ions will selectively substitute isovalent manganese cations in octahedral coordination ($Mn^{4+}O_6$). This assumption is consistent with the existence of the proper tin phase $CaCu_3Sn_4O_{12}$, which is isostructural to manganite $CaCu_3Mn_4O_{12}$ in which all octahedral positions are occupied by Sn^{4+} cations.[10]

The first component, Sn(1), with the highest hyperfine field value (Table I) evidently corresponds to the Sn^{4+} cations surrounded by six Mn^{4+} ions and six Cu^{2+} ions, so the experimentally observed $H_{Sn(1)}$ value can be represented by the sum of two groups of partial contributions as follows:

$$H_{Sn(1)} = 6h_{Mn} + 6h_{Cu}, \tag{6}$$

where h_{Mn} and h_{Cu} are the partial contributions to $H_{Sn(1)}$ from the Mn^{4+} and Cu^{2+} ions linked with tin by indirect Sn-O-Mn and Sn-O-Cu bonds. As will be clear below, the sign and magnitude of the resulting field $H_{Sn(1)}$ relate to (i) the electronic configuration of magnetic ions (Mn^{4+} and Cu^{2+}), (ii) the degree of covalence of Mn^{4+}-O and Cu^{2+}-O bonds, and (iii) the ϑ angles in the Sn-O-Mn and Sn-O-Cu chains.

The second Zeeman sextet Sn(2) can be attributed to the tin atoms in which nearest surrounding one of six manganese ions is replaced by the Sn^{4+} cation. Taking into account an additivity of the contributions to the hyperfine field H_{Sn} from the nearest magnetic ions, the difference in the hyperfine fields $H_{Sn(1)}$–$H_{Sn(2)} \approx 25$ kOe will correspond to the partial contribution of one Mn^{4+} ion to the magnetic hyperfine field $H_{Sn(1)}$. It is worth noting that the experimental relative intensity of the Sn(2) component ($I_2 \sim 30\%$) is well above the theoretical value (~6%) calculated using a binomial law, which implies a statistically uniform distribution of atoms. Such a discrepancy can indicate that our synthesis conditions do not provide a completely uniform distribution of impurity tin atoms over the octahedral sublattice of the sample. The tendency to form the Sn-O-Sn bonds is consistent with the existence of the tin phase $CaCu_3Sn_4O_{12}$.[10]

According to the scheme in Fig. 8(a), the partial field $h_{Cu} = h^{\sigma}_{Cu}$ caused by the $Cu^{2+}(b^1_{1g})$ cation with only one unpaired electron in the $3d$ orbital forming a σ bond with the $2p$ orbital of oxygen has the same direction as the total spin $S_{Cu} = 1/2$ of the copper cation. When the hyperfine field is induced by the $Mn^{4+}(t^3_{2g}e^0_g)$ cation, the situation is more complicated since an electron from the $2p$ orbital of the oxygen anion can be transferred either to the vacant e_g orbitals (σ bond) or to half-filled t_{2g} orbitals (π bond) of manganese [Fig. 8(b)]. According to the Hund rule, the electron transferred to the empty e_g orbital must have the same spin direction as the total spin of the Mn^{4+} ($S_{Mn} = 3/2$) cation. In this case, the unpaired electron remaining in the $2p$ orbital of the O^{2-} anion induces the partial field $h^{\sigma}_{Mn} < 0$ at the ^{119}Sn nuclei directed in an opposite direction to that of the total spin of the Mn^{4+} cation inducing this field. If an electron is transferred to the half-filled t_{2g} orbitals of Mn^{4+}, the electron remaining at oxygen will have the positive spin direction and, hence, the partial field induced

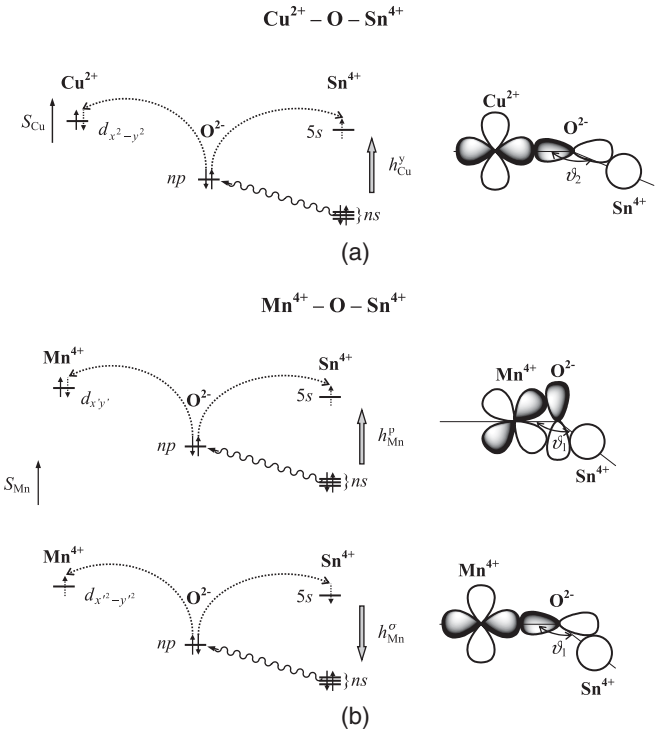

FIG. 8. Schematic diagram for the mechanism of inducing partial hyperfine magnetic field h_{Cu} by Cu^{2+} cations (a) and h_{Mn} by Mn^{4+} cations (b) (the wavy line corresponds to overlapped orbitals).

by this electron $h^{\pi}_{Mn} > 0$ also must have a positive direction (with respect to the S_{Mn} direction) [Fig. 8(b)].

It should be noted that, in addition to the different signs, the h^{σ}_{Mn} and h^{π}_{Mn} contributions depend differently on the ϑ_1 angle value. As follows from the scheme in Fig. 8(b), the $t_{2g} \overset{\pi}{-} p \overset{\sigma}{-} ns$ overlap in the Mn-O-Sn chain is the most efficient and, hence, the field h^{π}_{Mn} induced by this overlap is maximal at $\vartheta_1 = 90^\circ$. Conversely, spin density transfer due to the $e_g \overset{\sigma}{-} p \overset{\sigma}{-} ns$ overlap is most efficient at $\vartheta_1 = 180^\circ$. Thus, the sign and magnitude of the resulting contribution $h_{Mn} = h^{\sigma}_{Mn} + h^{\pi}_{Mn}$ is determined by the overlap of the orbitals involved in the σ and π bonds and, hence, by the value of the indirect bond angle ϑ_1 in the Mn-O-Sn chain.

The value of $h_{Mn} = h^{\sigma}_{Mn}(<0) + h^{\pi}_{Mn}(>0) \approx 34$ kOe obtained on model calculations (see Sec. IV) is qualitatively consistent with the experimental value $H_{Sn(1)} - H_{Sn(2)} \approx 25$ kOe (Table I), which, as we assume, is equal to the partial contribution to H_{Sn} from one Mn^{4+} cation. The observed discrepancy between the calculated and experimental values can be due to the nonadditivity of the contribution to H_{Sn} from the nearest cationic environment of tin caused by a change in the degree of electron transfer and overlap of wave functions on the substitution of Sn^{4+} for Mn^{4+}. The positive sign of the calculated h_{Mn} value shows that, in $CaCu_3Mn_{3.96}{}^{119}Sn_{0.04}O_{12}$ (at a given ϑ_1 angle of the indirect exchange bond in the Sn-O-Mn chain), the magnetic hyperfine field at ^{119}Sn nuclei is mainly induced due to electrons localized in the t_{2g} orbitals of manganese.

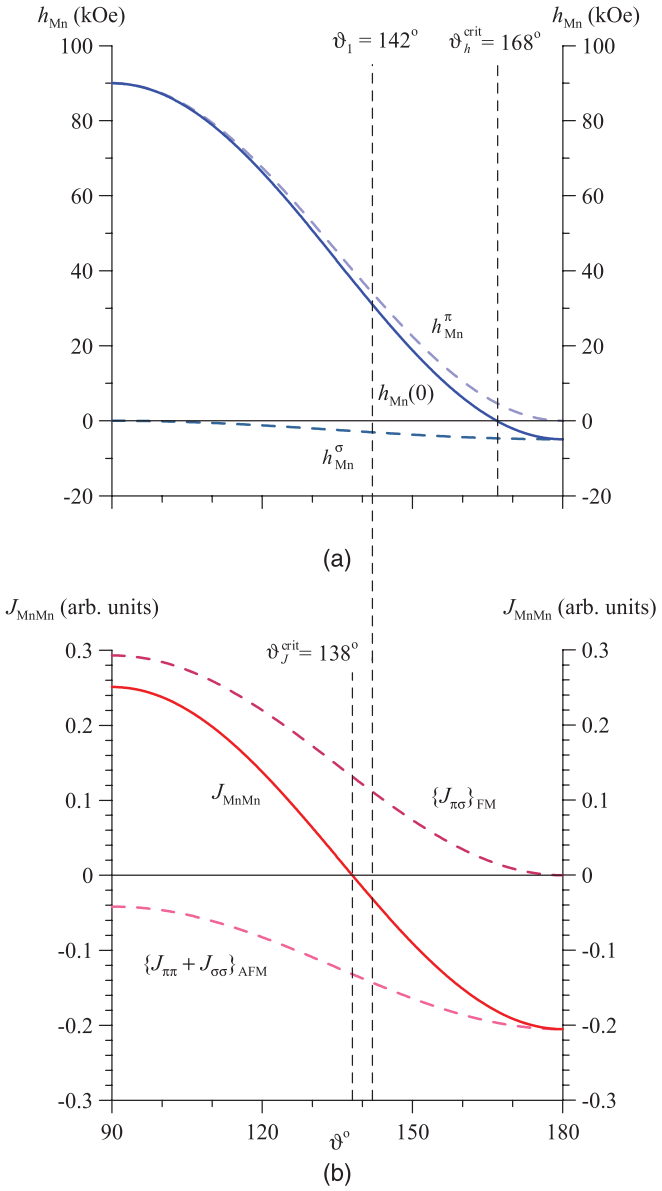

FIG. 9. (Color online) Angular dependencies of the contributions h^{π}_{Mn} and h^{σ}_{Mn} to the partial field h_{Mn} (a) and the various contributions to the exchange integral J_{MnMn} (b).

Using Eq. (1), we can estimate the critical value ϑ_h^{crit} of ϑ_1 angle at which $h^{\sigma}_{Mn} \approx h^{\pi}_{Mn}$, i.e., the overall partial contribution h_{Mn} changes its sign [Fig. 9(a)]:

$$\cos\vartheta_{crit} = -\left(\frac{(a^{\uparrow}_{\pi,Mn})^2}{(a^{\downarrow}_{\sigma,Mn})^2 - (a^{\uparrow}_{\sigma,Mn})^2 + (a^{\uparrow}_{\pi,Mn})^2}\right)^{1/2}. \quad (7)$$

It is worth noting that the value $\vartheta_h^{crit} = 168^\circ$, calculated by this equation, is rather close to the assumed value $\vartheta \sim 140^\circ$ (see below) at which indirect exchange interactions Mn^{4+}-O-Mn^{4+} become ferromagnetic.

To determine the sign of the partial contribution $h_{Cu} = h^{\sigma}_{Cu}$ from one Cu^{2+} cation to the total field H_{Sn}, we have to take into account that the spins of Mn^{4+} and Cu^{2+} cations are involved in antiferromagnetic exchange coupling Cu^{2+}-O-Mn^{4+}. Based on the symmetry and spatial distribution of the $3d$ orbitals of

these cations (Fig. 7), we can assume that their interaction is due to the overlap of the half-filled $d_{x^2-y^2}$ (b_{1g}) orbital of the Cu^{2+} cation (forming σ bonds with the $2p$ orbitals of the four nearest O^{2-} anions) and one of the three $d_{x'z'}$, $d_{y'z'}$, and $d_{x'y'}$ orbitals of the Mn^{4+} cation (forming π bonds with the $2p$ orbitals of six O^{2-} anions). According to the GKA rules,[24] indirect interactions involving the half-filled $3d$ orbitals should lead to antiferromagnetic ordering of the spins of interacting cations. Thus, the spins of the Mn^{4+} and Cu^{2+} cations in $CaCu_3Mn_4O_{12}$ are involved in antiferromagnetic π/σ interaction $t_{2g} \overset{\pi}{-} p \overset{\sigma}{-} d_{x^2-y^2}$. This means that the partial contribution $h_{Cu} = h^{\sigma}_{Cu}(< 0)$ should be opposite in sign to the above contribution $h_{Mn}(> 0)$ from one Mn^{4+} cation.

The substitution of the contributions $h_{Mn} = h^{\sigma}_{Mn} + h^{\pi}_{Mn}$ (> 0) and $h_{Cu} = h^{\sigma}_{Cu}$ (< 0) thus calculated into Eq. (6) leads to the hyperfine field $H_{Sn(1)} \approx 100$ kOe, which is close to the experimentally determined value of ≈105 kOe (Table I). Our calculations show that the magnetic structure suggested earlier on the basis of neutron diffraction data, as well as the above mechanism of inducing magnetic fields H_{Sn}, is consistent with the experimentally determined parameters of hyperfine coupling of ^{119}Sn nuclei in manganite $CaCu_3Mn_4O_{12}$.

B. Magnetic exchange interactions in $CaCu_3Mn_{3.96}{}^{119}Sn_{0.04}O_{12}$

Figure 10(a) shows the temperature dependence of the hyperfine field H^{max}_{Sn} corresponding to the maximum value of the $p(H_{Sn})$ distribution, which corresponds to the hyperfine field at the ^{119}Sn nuclei surrounded by six Mn^{4+} ions and six Cu^{2+} ions [see Eq. (6)]. Taking into account that the partial contributions $h_{Mn}(T)$ and $h_{Cu}(T)$ are due to the spin polarization of the ns orbitals of the tin cations by the neighboring Mn^{4+} and Cu^{2+} cations, the temperature-induced changes in each of them should be related to the temperature dependence of the reduced magnetizations $\sigma_{Mn}(T)$ and $\sigma_{Cu}(T)$ of the corresponding magnetic sublattices. The temperature dependencies of these magnetizations can be described in the framework of the Weiss local molecular field theory:[25]

$$\sigma_{Mn}(T) = B_{3/2}\left(2S_{Mn}\frac{z_{Mn(Mn)}J_{MnMn}S_{Mn}\sigma_{Mn}(T) + z_{Mn(Cu)}J_{MnCu}S_{Cu}\sigma_{Cu}(T)}{k_BT}\right), \tag{8a}$$

$$\sigma_{Cu}(T) = B_{1/2}\left(2S_{Cu}\frac{z_{Cu(Mn)}J_{CuMn}S_{Mn}\sigma_{Mn}(T)}{k_BT}\right), \tag{8b}$$

where $B_S(\ldots)$ is the Brillouin function for the spins $S_{Mn} = 3/2$ and $S_{Cu} = 1/2$; J_{MnMn} and $J_{CuMn} = J_{MnCu}$ are the indirect exchange coupling integrals for Mn^{4+}-O-Mn^{4+} and Cu^{2+}-O-Mn^{4+}, respectively; k_B is the Boltzmann constant; $z_{Mn(Mn)}$ and $z_{Mn(Cu)}$ are the numbers of, respectively, the Mn^{4+} and Cu^{2+} cations in the environment of a manganese cation; and $z_{Cu(Mn)}$ is the number of Mn^{4+} cations in the environment of a copper cation. For the chemical composition of the $CaCu_3Mn_{3.96}Sn_{0.04}O_{12}$ manganite, these numbers should be taken to be $z_{Mn(Mn)} = z_{Cu(Mn)} = 5.94$ and $z_{Mn(Cu)} = 6$.

Assuming that the magnetic moments of the Mn^{4+} and Cu^{2+} cations are collinear,[4] we can express their reduced overall magnetization $\sigma(T)$ through the reduced magnetizations $\sigma_{Mn}(T)$ and $\sigma_{Cu}(T)$ of the corresponding sublattices:

$$\sigma(T) = \frac{1}{n_{Mn}S_{Mn} - n_{Cu}S_{Cu}}[n_{Mn}S_{Mn}\sigma_{Mn}(T) + n_{Cu}S_{Cu}\sigma_{Cu}(T)], \tag{9}$$

where $n_{Mn} = 3.96$ and $n_{Cu} = 3$ are the numbers of the manganese and copper atoms per formula unit.

Inasmuch as the $h_{Mn}(T)$ and $h_{Cu}(T)$ partial contributions are proportional to the magnetic moments of the nearest neighbors of the tin probe atoms, i.e., manganese and copper cations for which one of the six magnetically active indirect bonds is replaced by the bond to a diamagnetic atom, these contributions can be calculated by the following equations:

$$\frac{h_{Mn}(T)}{|h_{Mn}(0)|} = B_{3/2}\left(2S_{Mn}\frac{(z_{Mn(Mn)} - 1)J_{MnMn}S_{Mn}\sigma_{Mn}(T) + z_{Mn(Cu)}J_{MnCu}S_{Cu}\sigma_{Cu}(T)}{k_BT}\right) \tag{10a}$$

$$\frac{h_{Cu}(T)}{|h_{Cu}(0)|} = B_{1/2}\left(2S_{Cu}\frac{(z_{Cu(Mn)} - 1)J_{CuMn}S_{Mn}\sigma_{Mn}(T)}{k_BT}\right). \tag{10b}$$

The set of Eqs. (8)–(10) makes it possible to describe the experimental temperature dependencies of the manganite hyperfine magnetic field $H_{Sn}(T)$ [Fig. 10(a)] and magnetization $\sigma(T)$ [Fig. 10(b)], with the exchange integrals J_{MnMn} and J_{CuMn} being fitting parameters. The same figures show the calculated $H_{Sn}(T)$ and $\sigma(T)$ plots obtained for the exchange integrals $J_{MnMn}/k_B = -0.6 \pm 0.2$ K and $J_{CuMn}/k_B = -51.1 \pm 0.3$ K, as well as the contributions of the corresponding sublattices to the hyperfine magnetic field and magnetization [see insets in Figs. 10(a) and 10(b)]. To better describe the

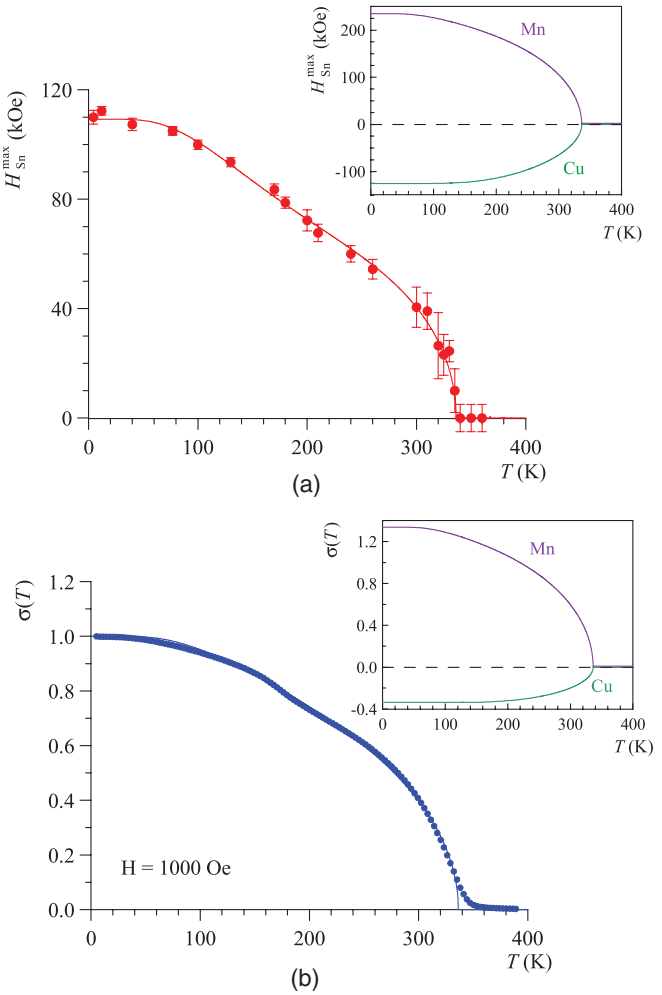

FIG. 10. (Color online) Temperature dependence of the hyperfine magnetic field H_{Sn}^{max} corresponding to the maximum value of the distribution $p(H_{Sn})$: the dots and the curve represent the experiment and the calculation, respectively. The inset shows the calculated temperature dependencies of the partial contributions to the hyperfine field H_{Sn} from the manganese and copper atoms (a). Temperature dependence of the reduced magnetization σ for the $CaCu_3Mn_{3.96}{}^{119}Sn_{0.04}O_{12}$ manganite in a field H = 1000 Oe: the dots and the curve represent the experiment and the calculation, respectively. The inset shows the calculated temperature dependencies of the partial contributions to the reduced magnetization from the manganese and copper atoms (b).

experimental $H_{Sn}(T)$ data at low temperatures ($T \to 0$), the partial contributions were corrected: $h_{Mn}(0) = 40$ kOe and $h_{Cu}(0) = -22$ kOe; however, they remain very close to the corresponding theoretical values.

The considerable difference between the exchange integral values, $|J_{CuMn}| \gg |J_{MnMn}|$, points to the dominant role of intersublattice Cu(↓)-O-Mn(↑) antiferromagnetic interactions in formation of the manganite magnetic structure. The J_{CuMn}/k_B value that we obtained is smaller than the value predicted at the functional density theory level, $J_{CuMn} = -20$ meV,[5] but considerably exceeds typical values for the exchange integrals of indirect magnetic coupling involving other $3d$-metal cations (5–30 K).[26] Such a discrepancy is likely due to the anomalously high, for oxide compounds, degree of covalence of Cu-O bonds formed by the Cu^{2+} cations with the square-planar oxygen coordination in the $CaCu_3Mn_4O_{12}$ structure.

It is worth noting that the J_{MnMn} exchange integral has a small negative magnitude, which is evidence of the weak antiferromagnetic character of the Mn^{4+}-O-Mn^{4+} intrasublattice indirect interactions. This result is seemingly inconsistent with the electronic configuration of Mn^{4+} cations (t_{2g}^3), for which overlap of half-filled t_{2g} orbitals should lead to strong antiferromagnetic coupling. This can be demonstrated by perovskite oxides $CaMnO_3$ (T_N = 123 K, $J_{MnMn}/k_B \approx -10$ K)[27] and $SrMnO_3$ ($T_N = 233$ K, $J_{MnMn}/k_B \approx -16$ K)[28] in which antiferromagnetic ordering of Mn^{4+} magnetic moments is exclusively due to Mn^{4+}-O-Mn^{4+} indirect π bonds. This puzzle could be resolved if we take into account the specificity of the electronic configuration of octahedrally coordinated Mn^{4+} cations ($t_{2g}^3 e_g^0$). Indeed, according to the GKA rules, when the ϑ angle in Mn-O-Mn chains tends to 180°, the antiferromagnetic π/π interaction $t_{2g} \overset{\pi}{-} p \overset{\pi}{-} t_{2g}$ involving the half-filled t_{2g} orbitals of manganese cations should dominate [Fig. 11(a)]. In addition to the indirect π/π interaction (which depends only slightly on the ϑ angle), the antiferromagnetic indirect σ/σ interaction $e_g \overset{\sigma}{-} p \overset{\sigma}{-} e_g$ involving the empty e_g orbitals, referred to as *semicovalent exchange*,[24] should be taken into account [Fig. 11(a)]. Theoretical estimates show that, as the angle ϑ decreases to 90°, the σ/π interaction $e_g \overset{\sigma}{-} p \overset{\pi}{-} t_{2g}$ between the vacant e_g orbitals and half-filled t_{2g} orbitals of Mn^{4+} cations [Fig. 11(b)] can give a significant ferromagnetic contribution to the exchange interactions Mn^{4+}-O-Mn^{4+}. It can be assumed that, below the critical value (ϑ_J^{crit}), the σ/π interaction can be so strong that magnetic order of the spins in the Mn-O-Mn chains change its sign and becomes ferromagnetic. However, no oxygen-containing system has been found so far in which the existence of the indirect σ/π interaction leading to ferromagnetic order of Mn^{4+} cations was proved. In order to verify this assumption we calculate the angular dependence of the exchange Mn^{4+}-O-Mn^{4+} interactions each of which consists of two π/π interactions, one σ/σ interaction, and two σ/π interactions.

According to the perturbation theory,[29] the antiferromagnetic (AF) π/π interactions $t_{2g} \overset{\pi}{-} p \overset{\pi}{-} t_{2g}$ involving the half-filled t_{2g} orbitals of manganese cations [Fig. 11(a)] can be expressed as

$$\left\{J_{\pi\pi}^{kin} + J_{\pi\pi}^{semicov}\right\}_{AF} \propto \frac{t_{pd\pi}^4}{\Delta_\pi^2}\left(\frac{4}{U_d} + \frac{8}{2\Delta_\pi + U_p}\right)\left(1 - \frac{1}{2}\sin^2\vartheta\right), \quad (11)$$

where $t_{pd\pi}$ is the cation-anion electron-energy transfer integral corresponding to the π/π interactions; U_d is the on-site electron-electron Coulomb energy required to excite an electron from one d^3 manifold to another; U_p is the Coulomb repulsion energy between two holes on the same oxygen ion; and Δ_π is the energy to excite an electron from an $2p_\pi(O^{2-})$ orbital to the lowest unoccupied d orbital of d^3 manifold. The first term in Eq. (11) corresponds to the conventional Anderson kinetic superexchange ($J_{\pi\pi}^{kin}$), and the second is the semicovalent exchange ($J_{\pi\pi}^{semicov}$) associated with the transfer of two electrons from the same oxygen $2p_\pi$ orbital, one to Mn^{4+} on one side and the other to the Mn^{4+} cation on the opposite side of the O^{2-} ion.[29] The spin of the

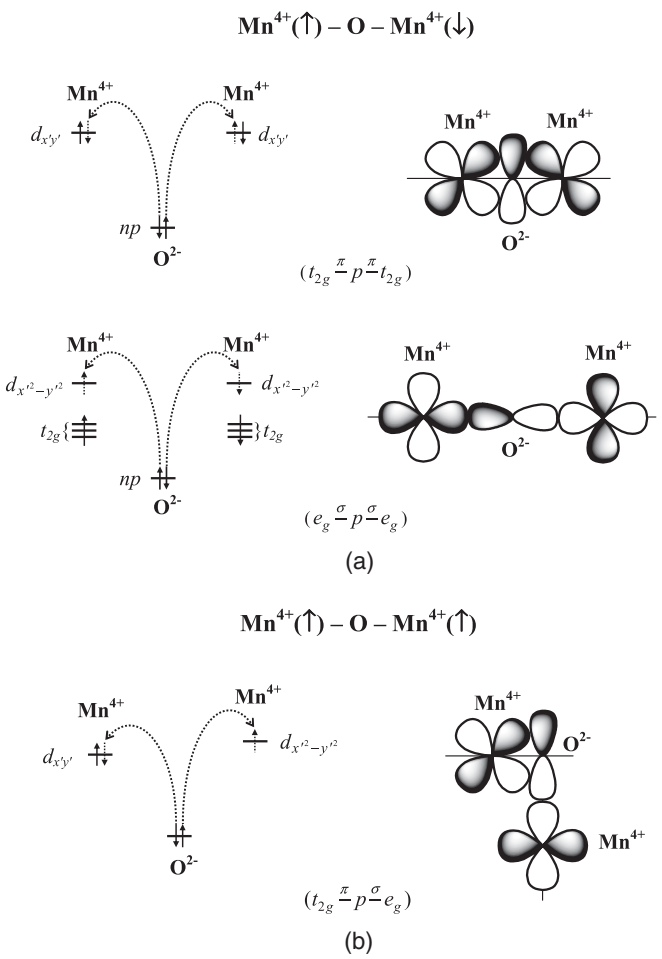

FIG. 11. Relative position of the $3d$ orbitals of Mn^{4+} cations and the $2p$ orbitals of O^{2-} anions (for the case of their maximum overlapping) that results in an antiferromagnetic (a) and ferromagnetic (b) interactions in the Mn-O-Mn chains and the schematic diagram illustrating the application of the Goodenough-Kanamori-Anderson rules.

transferred electron is conserved, and the Pauli exclusion principle restricts transfer to a state antiparallel to the spin on the acceptor cation.

In the case of the $e_g \overset{\sigma}{-} p \overset{\sigma}{-} e_g$ interaction, the two empty e_g orbitals of manganese cations [Fig. 11(a)] give an antiferromagnetic σ bond spin-spin interaction via a purely semicovalent exchange ($J_{\sigma\sigma}^{\text{semicov}}$), which can be expressed as

$$\left\{J_{\sigma\sigma}^{\text{semicov}}\right\}_{\text{AF}} \propto \frac{t_{pd\sigma}^4}{\Delta_\sigma^2} \frac{2J_H^{Mn}}{(2\Delta_\sigma + U_p)^2} \cos^2\vartheta, \tag{12}$$

where Δ_σ is the energy to excite an electron from an $2p_\sigma(O^{2-})$ orbital to the unoccupied e_g orbital of the Mn^{4+} cation; J_H^{Mn} is the intra-atomic Hund's energy. In the case of the Mn^{4+} cations having three electrons with parallel spins, the Hund's energy equals to triple usual atomic value of $J_H \sim 0.8$ eV for $3d$ metal series with total spin $S = 1$. Since the two $2p_\sigma(O^{2-})$ orbitals have antiparallel spins by the Pauli exclusion principle and intra-atomic ferromagnetic exchange of the manganese cations stabilizes transfer of a spin parallel to the preexisting t_{2g}^3 spins, the virtual transfer of opposite spins from the same $2p_\sigma(O^{2-})$ orbital couples the two Mn^{4+} cation spins antiferromagnetically.

The last $e_g \overset{\sigma}{-} p \overset{\pi}{-} t_{2g}$ contribution to the total Mn^{4+}-O-Mn^{4+} exchange interaction is coming from the virtual hopping from the occupied t_{2g} to the empty e_g orbital, as shown in [Fig. 11(b)]. Since Hund's rule coupling J_H^{Mn} tends to orient spins at an ion parallel, this σ/π contribution will result in ferromagnetic (FM) exchange,

$$\left\{J_{\sigma\pi}^{\text{kin}} + J_{\sigma\pi}^{\text{semicov}}\right\}_{\text{FM}} \propto \frac{t_{pd\sigma}^2 t_{pd\pi}^2}{\Delta_\sigma \Delta_\pi} \left(\frac{4J_H^{\text{Mn}}}{U_d^2} + \frac{8J_H^{\text{Mn}}}{(\Delta_\sigma + \Delta_\pi + U_p)^2}\right) \sin^2\vartheta. \tag{13}$$

To our knowledge, there are not yet photoemission experiments nor constrained calculations yielding the $t_{pd\sigma(\pi)}$, $\Delta_{\sigma(\pi)}$, U_d, and U_p energies for the $CaCu_3Mn_4O_{12}$ perovskite. Therefore, these parameters were taken as an average in wide variety of values for Mn^{4+} cations presented in the literature: $t_{pd\sigma} = 1.5$ eV, $t_{pd\pi} = 0.7$ eV, $\Delta_\sigma \approx \Delta_\pi = 2$ eV, $U_d = 7.8$ eV, and $U_p = 1$ eV.

According to the angular dependence of exchange integrals Eqs. (11)–(13), at Mn-O-Mn angles close to 180°, the coupling of Mn^{4+} cations will be antiferromagnetic. With an increase in the angle ϑ ($\rightarrow 90°$), coupling first becomes weaker and then, at a certain critical value $\vartheta_J^{\text{crit}}$, changes the sign and becomes ferromagnetic. The $\vartheta_J^{\text{crit}}$ value can be estimated from the following equality:

$$\left\{J_{\pi\pi}^{\text{kin}} + J_{\pi\pi}^{\text{halfcov}}\right\}_{\text{A}\Phi} + \left\{J_{\sigma\sigma}^{\text{halfcov}}\right\}_{\text{A}\Phi} = \left\{J_{\sigma\pi}^{\text{kin}} + J_{\sigma\pi}^{\text{halfcov}}\right\}_{\text{FM}}. \tag{14}$$

The substitution of all necessary parameters and the solution of Eq. (14) into Eqs. (11)–(13) gave the critical angle value $\vartheta_J^{\text{crit}} = 138°$, which is rather close to $\vartheta_1 = 142°$ corresponding to the Mn-O-Mn angle in unsubstituted manganite.[4] Despite the absence of reliable experimental values of the parameters in Eqs. (11)–(13), the estimated value ($\vartheta_J^{\text{crit}} \approx \vartheta_1$) is a semiquantitative proof that the Mn-O-Mn angle in the $CaCu_3Mn_4O_{12}$ structure falls within the range of values [Fig. 9(b)] at which antiferromagnetic interactions between the manganese cations first become weaker ($\vartheta \geqslant \vartheta_J^{\text{crit}}$) and then change the sign and become ferromagnetic ($\vartheta \leqslant \vartheta_J^{\text{crit}}$).

According to our results, despite a weak antiferromagnetic Mn^{4+}-O-Mn^{4+} interactions ($J_{\text{MnMn}} < 0$), it is mainly the Cu^{2+}-O-Mn^{4+} couplings which force the Mn^{4+} spins to be parallel, inducing some frustration in the octahedral B sublattice. This conclusion is well corroborated with magnetic data for another double perovskites: $CaCu_{2.5}Mn_{4.5}O_{12}$[6] and $TbCu_3Mn_4O_{12}$.[30] The observed decrease of the Curie temperature for $CaCu_{2.5}Mn_{4.5}O_{12}$ ($T_C = 345$ K)[6] is due to stabilization of the trivalent $(Mn^{3+})_A$ cations at the A positions together with Cu^{2+} cations. Taking into account that the $(Mn^{3+})_A$ cations are coupled to octahedral $(Mn^{3+}/Mn^{4+})_B$ ones by much weaker interactions, such stabilization increases the competition/frustration between A-B and B-B couplings [the $(Mn)_B$ spins adopt a noncolliner configuration to minimize frustration effects].[6] The ferrimagnet $TbCu_3Mn_4O_{12}$ has a higher Curie temperature $T_C = 395$ K[30] with respect to the $CaCu_3Mn_4O_{12}$. This may be a result of the electronic

injection $(Mn^{4+} \rightarrow Mn^{3+})_B$ in octahedral B sublattice on Ca^{2+} replacement by Tb^{3+} cations, reinforcing the ferromagnetic contribution in octahedral manganese sublattice due to the double exchange mechanism between $(Mn^{3+})_B$ and $(Mn^{4+})_B$ cations.[30]

It may seem unusual that, despite the weak exchange coupling Mn^{4+}-O-Mn^{4+} ($J_{MnMn}/k_B = -0.6$ K), the partial contribution to the hyperfine magnetic field at the Sn^{4+} nuclei made by each of the surrounding Mn^{4+} cations [$h_{Mn}(0) = 40$ kOe] noticeably exceeds the corresponding $h_{Cu}(0) = -2$ kOe contribution of the copper cations. Like the exchange integral J_{MnMn}, the $h_{Mn}(0)$ quantity can be represented as a superposition of the h^{π}_{Mn} and h^{σ}_{Mn} contributions of opposite sign, having different angular dependencies [Fig. 9(a)]. However, as distinct from the exchange integrals [Fig. 9(b)], the critical value $\vartheta_h^{crit} = 168^\circ$ at which $h^{\pi}_{Mn} \approx h^{\sigma}_{Mn}$, i.e., the overall partial contribution h_{Mn} changes the sign, is considerably higher than $\vartheta_1 = 142^\circ$. The physical reason for this is a considerable difference between the covalence parameters $(a^{\uparrow}_{\sigma,Mn})^2 - (a^{\downarrow}_{\sigma,Mn})^2 = -0.008$ and $(a^{\uparrow}_{\pi,Mn})^2 = 0.167$ corresponding to the σ and π Mn-O bonds.

VI. CONCLUSIONS

In summary, by means of ^{119}Sn probe Mössbauer spectroscopy, we have shown how information about strength and sign of the superexchange interactions in perovskite $CaCu_3Mn_{3.96}{}^{119}Sn_{0.04}O_{12}$ can be obtained from an analysis of supertransferred hyperfine interactions of tin probe ions. It has been demonstrated that

(a) the probe tin atoms are stabilized in the manganite structure with the formal oxidation state "+4" by substituting for Mn^{4+} cations in the octahedral oxygen environment;

(b) the magnetic hyperfine field H_{Sn} at the nuclei of Sn^{4+} cations is a superposition of partial contributions $h_{Mn}(>0)$ and $h_{Cu}(<0)$ of different sign due to spin transfer involving the Mn^{4+} and Cu^{2+} cations from different structural sublattices;

(c) not only intersublattice antiferromagnetic interactions $Cu^{2+}(\downarrow)$-O-$Mn^{4+}(\uparrow)$ but also intrasublattice ferromagnetic interactions $Mn^{4+}(\uparrow)$-O-$Mn^{4+}(\uparrow)$ play a noticeable role in the formation of the magnetic structure of $CaCu_3Mn_4O_{12}$; as in other perovskite-like manganites, the magnitude and sign of indirect exchange coupling between octahedrally coordinated Mn^{4+} cations depend on the angle in the Mn-O-Mn chains and the covalence parameters of Mn^{4+}-O chemical bonds.

ACKNOWLEDGMENTS

The authors thank the valuable discussions with D. I. Khomskii. This work was supported by the Russian Foundation for Basic Research, Project No. 08-02-00354-a.

APPENDIX

The supertransferred hyperfine field H_{Sn} is caused by the overlap distortions of doubly occupied ns-orbitals (n = 1–4) and spin transfer into the empty $5s$-orbital of the Sn^{4+} cations by the ligand orbitals which have been unpaired by transfer into unoccupied $3d$-orbitals of the neighboring magnetic (M^{m+}) cations. The basic theoretical principles of the supertransferred hyperfine interactions which were developed in Refs. 12–14 are in many respects analogous to that accepted in the theory of superexchange.

To obtain H_{Sn} we consider the central Sn^{4+} cation surrounded by six oxygen ions, each of which has a magnetic M^{m+} ($= Cu^{2+}$ or Mn^{2+}) cation as a nearest neighbor. Molecular orbitals of the $\{$Sn-6O-$(zM)\}$ cluster may be constructed on the basis of atomic (filled or empty) orbitals: $3d$ orbitals of the magnetic M^{m+} cations; ns orbitals (n = 1–5) of the nonmagnetic Sn^{4+} cation; and $2p$ orbitals of the O^{2-} ions. *Sawatzky* with coworkers[12] have taken into account the contribution from the bonding $\Psi_O^{\uparrow(\downarrow)}$molecular orbitals, which have the same symmetry (A_{1g}) as the ns orbitals of the central Sn^{4+} cation:

$$\Psi_O^{\uparrow(\downarrow)} = N_O^{\uparrow(\downarrow)} \left(\chi_{2p}^{\uparrow(\downarrow)} + \sum_k^z D_k^{\uparrow(\downarrow)} \varphi_{3d}^{\uparrow(\downarrow)} + B_{5s}^{\uparrow(\downarrow)} \phi_{5s}^{\uparrow(\downarrow)} - \sum_{n=1}^{4} S_{ns}^{\uparrow(\downarrow)} \phi_{ns}^{\uparrow(\downarrow)} \right), \quad \text{(A1)}$$

where $\chi_{2p}^{\uparrow(\downarrow)}$ is a combination of the $2p$ orbitals of the O^{2-} ions; $\phi_{ns}^{\uparrow(\downarrow)}$ and $\phi_{5s}^{\uparrow(\downarrow)}$ are ns orbitals (n = 1–5) of the Sn^{4+} cation; $\varphi_{3d}^{\uparrow(\downarrow)}$ is a combination of the $3d$ orbitals of the neighboring M^{m+} cations; $B_{5s}^{\uparrow(\downarrow)}$ is group $2p^6(O^{2-}) \rightarrow 5s^0(Sn^{4+})$ transfer integral and $S_{ns}^{\uparrow(\downarrow)} = \langle \chi_{2p}^{\uparrow(\downarrow)} \mid \phi_{ns}^{\uparrow(\downarrow)} \rangle$ are group overlap integrals which, for octahedral symmetry of the $\{Sn^{4+}$-(O-$M^{m+})_6\}$ clusters, are related with the proper single bond $b_{5s}^{\uparrow(\downarrow)}$ and $s_{ns}^{\uparrow(\downarrow)}$ integrals:

$$B_{5s}^{\uparrow(\downarrow)} = \sqrt{6} b_{5s}^{\uparrow(\downarrow)} \text{ and } S_{ns}^{\uparrow(\downarrow)} = \sqrt{6} s_{ns}^{\uparrow(\downarrow)}. \quad \text{(A2)}$$

Parameters $D_k^{\uparrow(\downarrow)}$ are introduced to consider the electron transfer from the filled $2p$ orbitals of the O^{2-} ions to the vacant $3d$ orbitals of the neighboring M^{m+} cations and the overlapping of the wave function of these ions as well. These parameters strongly depend on whether the $3d$ orbitals are filled or empty:

$$D_k^{\uparrow(\downarrow)} = \begin{cases} B_{3d}^{\uparrow(\downarrow)}, & \text{for empty } 3d \text{ orbitals} \\ -S_{3d}, & \text{for occupied } 3d \text{ orbitals} \end{cases},$$

where $B_{3d}^{\uparrow(\downarrow)}$ is the parameter describing the electron transfer $2p^6(O^{2-}) \rightarrow 3d(M^{m+})$ and $S_{3d}^{\uparrow(\downarrow)} = \langle \chi_{2p}^{\uparrow(\downarrow)} \mid \varphi_{3d}^{\uparrow(\downarrow)} \rangle$ is the overlap integral. According to Refs. 12–14, the product of these group integrals by $\varphi_{3d}^{\uparrow(\downarrow)}$ wave functions can be related with the transfer integrals ($b_\sigma^{\uparrow(\downarrow)}$ and $b_\pi^{\uparrow(\downarrow)}$) and the overlap integrals ($s_\sigma^{\uparrow(\downarrow)}$ and $s_\pi^{\uparrow(\downarrow)}$) of single σ and π bonds M^{m+}-O:

$$\begin{aligned} S_{3d}^{\uparrow(\downarrow)} \phi_{3d}^{\uparrow(\downarrow)} &= s_\sigma^{\uparrow(\downarrow)} \cos\vartheta (\phi_{3d,\sigma}^{\uparrow(\downarrow)}) - s_\pi^{\uparrow(\downarrow)} \sin\vartheta (\phi_{3d,\pi}^{\uparrow(\downarrow)}) \\ B_{3d}^{\uparrow(\downarrow)} \phi_{3d}^{\uparrow(\downarrow)} &= b_\sigma^{\uparrow(\downarrow)} \cos\vartheta (\phi_{3d,\sigma}^{\uparrow(\downarrow)}) - b_\pi^{\uparrow(\downarrow)} \sin\vartheta (\phi_{3d,\pi}^{\uparrow(\downarrow)}), \end{aligned} \quad \text{(A3)}$$

where ϑ is angle in the Sn-O-M chains.

The hyperfine field at the nucleus of the $^{119}Sn^{4+}$ ion

$$H_{Sn} = \frac{8\pi}{3} \mu_B \{ \Psi_O^{\uparrow 2}(0) - \Psi_O^{\downarrow 2}(0) \} \quad \text{(A4)}$$

is considerably dependent on the values of the normalization constants $N_O^{\uparrow}$ and $N_O^{\downarrow}$ for the molecular orbitals (A.1). The evaluation of these constants presents certain difficulties mainly due to the problem of the adequate description the ground-state electron configurations of the M^{m+} cations. In our case of the octahedral {Sn-6O-(6Mn)} and {Sn-6O-(6Cu)} clusters, containing the Mn^{4+} ($^4A_{1g}$) and Cu^{2+} ($^2B_{1g}$) cations with nondegenerate electronic configurations, the normalization constants are given by

$$N_O^{\uparrow} = \left[1 + S_{ZZ} - s_\sigma^2 \cos^2\vartheta - s_\pi^2 \sin^2\vartheta + 6b_{5s}^2 s_{5s} - 6\sum_{n=1}^{3}(s_{ns}^{\uparrow})^2\right]^{-1/2} \tag{A5}$$

$$N_O^{\downarrow} = \left[1 + S_{ZZ} + \left(b_\sigma^2 + 2b_\sigma s_\sigma\right)\cos^2\vartheta + \left(b_\pi^2 + 2b_\pi s_\pi\right)\sin^2\vartheta + 6b_{5s}^2 + 12b_{5s}s_{5s} - 6\sum_{n=1}^{3}(s_{ns}^{\downarrow})^2\right]^{-1/2}. \tag{A6}$$

In determining the normalization constants $N_O^{\uparrow}$ and $N_O^{\downarrow}$ we take into account the oxygen-oxygen overlap group $S_{zz} = \frac{1}{6}\sum_{i,j}\langle p_{z_i} \mid p_{z_j}\rangle$ integral.

The final expression for the partial contributions from the M^{m+} cations to the hyperfine field at the ^{119}Sn nucleus is given by

$$H_{Sn} = 525(N_O^{\uparrow}N_O^{\downarrow})^2\left(-\sum_{n=1}^{4}s_{ns}^{\uparrow(\downarrow)}\phi_{ns}^{\uparrow(\downarrow)}(0) + b_{5s}^{\uparrow(\downarrow)}\phi_{5s}^{\uparrow(\downarrow)}(0)\right)^2\sum_i z_i[(a_{\sigma,i}^{\uparrow(\downarrow)})^2\cos^2\vartheta_i + (a_{\pi,i}^{\uparrow(\downarrow)})^2\sin^2\vartheta_i], \tag{A7}$$

were $(a_{\sigma,i}^{\uparrow(\downarrow)})^2 = (b_{\sigma,i}^{\uparrow(\downarrow)} + s_{\sigma,i}^{\uparrow(\downarrow)})^2$ and $(a_{\pi,i}^{\uparrow(\downarrow)})^2 = (b_{\pi,i}^{\uparrow(\downarrow)} + s_{\pi,i}^{\uparrow(\downarrow)})^2$ are the commonly used covalency parameters, respectively, for σ and π bonds of the M^{m+} cation with surrounding O^{2-} ions; $\varphi_{ns}(0)$ are the wave functions of ns orbitals (n = 1–5) at the nuclei of Sn^{4+} cations.

[1] E. Dagotto, T. Hotta, and A. Moreo, Phys. Rep. **344**, 1 (2001).
[2] Z. Zeng, M. Greenblatt, M. A. Subramanian *et al.*, Phys. Rev. B **82**, 3164 (1999).
[3] A. Castro-Couceiro, S. Yáñez-Vilar, B. Rivas-Murias *et al.*, J. Phys. Condens. Matter **18**, 3803 (2006).
[4] Z. Zeng, M. Greenblatt, J. E. Sunstrom IV *et al.*, J. Solid State Chem. **147**, 185 (1999).
[5] R. Weht and W. E. Pickett, Phys. Rev. B **65**, 014415 (2001).
[6] J. Sánchez-Benitez, J. A. Alonso, M. J. Martinez-Lope *et al.*, Chem. Mater. **15**, 2193 (2003).
[7] V. S. Rusakov, I. A. Presnyakov, A. V. Sobolev *et al.*, Zh. Eksp. Teor. Fiz. **135**, 692 (2009) [JETP **108**, 605 (2009)].
[8] V. S. Rusakov, *Mössbauer Spectroscopy of Locally Inhomogeneous Systems* (Institute of Nuclear Physics, National Nuclear Center of the Republic of Kazakhstan, Almaty, 2000).
[9] J. Sánchez-Benitez, C. Prieto, A. de Andrés *et al.*, Phys. Rev. B **70**, 024419 (2004).
[10] H. Shiraki, T. Saito, T. Yamada *et al.*, Phys. Rev. B **76**, 140403(R) (2007).
[11] V. S. Rusakov and K. K. Kadyrzhanov, Hyperfine Interact. **164**, 87 (2005).
[12] F. van der Woude and G. A. Sawatzky, Phys. Rev. B **4**, 3159 (1971).
[13] A. S. Moskvin, N. S. Ovanesyan, and V. A. Trukhtanov, Hyperfine Interact. **3**, 429 (1977).
[14] I. A. Presnyakov, K. V. Pokholok, I. G. Minyaoelova *et al.*, Izv. Akad. Nauk, Ser. Fiz. **80**, 824 (1999).
[15] J. K. Lees and P. A. Flinn, J. Chem. Phys. **48**, 882 (1968).
[16] P. A. Flinn, in *Mössbauer Isomer Shift*, edited by G. K. Shenoy and F. E. Wagner (North-Holland, Amsterdam, 1978), p. 593.
[17] M. Takano, Y. Takeda, M. Shimada *et al.*, J. Phys. Soc. Jpn. **39**, 656 (1975).
[18] A. S. Moskvin, N. S. Ovanesyan, and V. A. Trukhtanov, Hyperfine Interact. **5**, 13 (1977).
[19] J. Owen and D. Taylor, J. Appl. Phys. **39**, 791 (1968).
[20] W. A. Harrison, *Electronic Structure and Properties of Solids* (Freeman, San Francisco, CA, 1980).
[21] J. Chenavas, J. C. Joubert, M. Marezio *et al.*, J. Solid State Chem. **14**, 25 (1975).
[22] A. E. Bocquet, T. Mizokawa, T. Saitoh *et al.*, Phys. Rev. B **46**, 3771 (1992).
[23] H. Falcón, J. Sánchez-Benitez, M. J. Martinez-Lope *et al.*, J. Phys. Condens. Matter **19**, 356209 (2007).
[24] J. B. Goodenough, *Magnetism and the Chemical Bond* (Interscience-Wiley, New York, 1963).
[25] J. M. D. Coey and G. A. Sawatzky, Phys. Status Solidi B **44**, 673 (1971).
[26] S. Krupichka, *Physik der Ferrite und der verwandten magnetischen Oxide* (Academia, Prague, 1973; Mir, Moscow, 1976), Vol. 1 [in German and in Russian].
[27] A. J. Millis, Phys. Rev. B **55**, 6405 (1997).
[28] O. Chmaissem, B. Dabrowski, S. Kolesnik *et al.*, Phys. Rev. B **64**, 134412 (2001).
[29] S. V. Streltsov and D. I. Khomskii, Phys. Rev. B **77**, 064405 (2008).
[30] J. Sánchez-Benitez, J. A. Alonso, A. De Andres, M. J. Martinez-Lope *et al.*, Chem. Mater. **17**, 5070 (2005).